Biological Procedures Online

RESEARCH

Open Access

Assessment and Evaluation of Contemporary Approaches for Astrocyte Differentiation from hiPSCs: A Modeling Paradigm for Alzheimer's Disease

Veronika Juráková[1], Balázs Széky[2], Martina Zapletalová[1], Anita Fehér[2], Melinda Zana[2], Shashank Pandey[3], Radek Kučera[3], Omar Šerý[1,4], Jiří Hudeček[6], András Dinnyés[2,5] and Jan Lochman[1,4*]

Abstract

Background Astrocytes have recently gained attention as key players in the pathogenesis of neurodegenerative diseases, including Alzheimer's disease. Numerous differentiation protocols have been developed to study human astrocytes in vitro. However, the properties of the resulting glia are inconsistent, making it difficult to select an appropriate method for a given research question. Therefore, we compared three approaches for the generation of iPSC-derived astrocytes. We performed a detailed analysis using a widely used long serum-free (LSFP) and short serum-free (SSFP) protocol, as well as a TUSP protocol using serum for a limited time of differentiation.

Results We used RNA sequencing and immunochemistry to characterize the cultures. Astrocytes generated by the LSFP and SSFP methods differed significantly in their characteristics from those generated by the TUSP method using serum. The TUSP astrocytes had a less neuronal pattern, showed a higher degree of extracellular matrix formation, and were more mature. The short-term presence of FBS in the medium facilitated the induction of astroglia characteristics but did not result in reactive astrocytes. Data from cell-type deconvolution analysis applied to bulk transcriptomes from the cultures assessed their similarity to primary and fetal human astrocytes.

Conclusions Overall, our analyses highlight the need to consider the advantages and disadvantages of a given differentiation protocol for solving specific research tasks or drug discovery studies with iPSC-derived astrocytes.

Keywords IPSC, Astrocytes, FBS, Disease modeling, Aβ42

*Correspondence:
Jan Lochman
jlochman@sci.muni.cz
[1] Department of Biochemistry, Faculty of Science, Masaryk University, Brno, Czech Republic
[2] BioTalentum Ltd, Godollo, Hungary
[3] Department of Pharmacology and Toxicology, Faculty of Medicine in Pilsen, Charles University, Prague, Czech Republic
[4] Laboratory of Neurobiology and Pathological Physiology, Institute of Animal Physiology and Genetics, The Czech Academy of Science, Veveří 97, 60200 Brno, Czech Republic
[5] Department of Physiology and Animal Health, Institute of Physiology and Animal Nutrition, Hungarian University of Agriculture and Life Sciences, Godollo, Hungary
[6] Psychiatric Clinic, University Hospital and Faculty of Medicine in Pilsen, Charles University, Pilsen, Czech Republic

Background

Astrocytes are now widely recognized as critical elements in maintaining neuronal homeostasis and defending against pathologies, including Alzheimer's disease (AD) [1]. Astrocytes express numerous homeostatic pathways that support the functional activity of the central nervous system and provide an important neuroprotective function. Astrocytes also produce substances that stimulate neurogenesis and synaptogenesis, thereby facilitating communication between neurons [2]. In addition, astrocytes and other neuroglial cells play a crucial role in the immune response of the central nervous system (CNS) and act as a primary defense system by regulating the volume and composition of the extracellular space. Astrocytes are also affected by pathological changes, such as those affecting neuronal cells.

Astrocytes play a role in the pathogenesis of neurodegenerative diseases such as AD, Parkinson's disease, and amyotrophic lateral sclerosis [1, 3, 4]. In patients with AD, astrocytes undergo complex changes, leading to both a loss of function and the accumulation of reactive cells. Reactive astrogliosis represents a defensive mechanism wherein astrocytes experience both morphological and functional transformations in response to brain injuries or diseases such as AD [5].

From the above, it follows that detailed research on astrocytes in both the normal brain and the brains of individuals with AD is crucial for understanding the pathogenesis of AD. Unfortunately, research on astrocytes using model organisms often fails to capture some pathological processes occurring in AD. Moreover, human astrocytes are much more complex and diverse, and their morphology significantly differs from that of rodent and primate astrocytes [6]. They exhibit notable ontogenetic and heterogenous characteristics, which are pivotal for their multifaceted functions. A comprehensive understanding of the development and identification of astrocytes through the use of specific markers across the various stages of their maturation is essential for the study of their role in the CNS. Astrocyte development has been observed to originate from the embryonic stage, with neural progenitor cells (NPCs) and radial glial cells (RGCs) serving as the initial differentiating cells into neurons. As neurogenesis declines, the same progenitors begin to give rise to astrocytes [7]. Nevertheless, the precise mechanisms underlying the gliogenic switch remain unclear. These include the activation of the Notch signaling pathway in radial glia [8], which promotes astrogenesis, and the stimulation of gliogenesis through stimulation of the JAK-STAT signaling pathway [9] by cytokine release by neurons and growth factors like bone morphogenetic proteins (BMPs) or ciliary neurotrophic factor (CNTF). Glutamate aspartate transporter (GLAST) and glial fibrillary acidic protein (GFAP) are pivotal markers in the initial stages of astrocyte development, followed by markers such as aldehyde dehydrogenase 1 family member L1 (Aldh1L1) and S100 calcium-binding protein B (S100β), which indicate the onset of specialized functions during the maturation of astrocytes. The most prominent markers in fully mature astrocytes are aquaporin-4 (AQP4), connexin-43 (Cx43), glutamate transporters excitatory amino acid transporters 1 and 2 (EAAT1/2), and GFAP, with expression varying by CNS region and functional requirements [10]. Although GFAP is an essential and commonly utilized marker for identifying astrocytes, its expression is markedly variable across diverse astrocyte cultures, different brain regions, and distinct astrocyte subgroups [11]. Furthermore, GFAP is also expressed by early glial progenitor cells, which give rise to both astrocytes and oligodendrocytes [12].

Despite the comprehensive description of the morphological diversity of astrocyte populations by Ramón y Cajal [13], astrocytes have historically been classified as fibrous or protoplasmic based on their location in white or gray matter, respectively. New technological approaches have revealed striking astrocyte diversity between and within brain regions. However, the diversity of astrocytes within a given brain region may be attributed to developmental patterning events and/or local adaptations of astrocytes to their environment [14]. This represents a continuum of transcriptional profiles rather than distinct subtypes. In response to CNS injury, neurodegeneration, or infection, astrocytes undergo rapid changes collectively referred to as astrocyte reactivity. To elucidate the diversity, regulation, and functions of astrocyte reactivity, two distinct types of reactive astrocytes have recently been characterized: the neurotoxic or pro-inflammatory phenotype (A1) and the neuroprotective or anti-inflammatory phenotype (A2) [15]. Rodríguez-Giraldo et al. (2022) [16] and Šerý et al. (2020) [17] review the dual role of astrocytes and microglia in the pathogenesis of AD, which can be both neuroprotective and neurotoxic, depending on the stage of AD and micro environmental factors. This impairment of the function of these glial cells may be one of the mechanisms leading to the primary lesion that contributes to the pathogenesis of AD.

In order to understand the intricate regulation of astrocyte reactivity during neuroinflammation, human induced pluripotent stem cell (hiPSC) technology offers an innovative and potentially ground-breaking means of exploring the essential mechanisms of CNS disease. Recently, multiple research teams have produced hiPSC-derived astrocytes; however, these methods remain challenging and require prolonged and/or technically

complex protocols [18, 19]. Currently, there are two basic approaches to astrocytes induction. The first method involves using fetal bovine serum (FBS) in the differentiation medium to initiate the differentiation of progenitor cells into astrocytes and reduce neuron formation [19, 20]. However, it has been suggested by other studies that the use of FBS during astrocyte induction may affect the phenotype, reactivity, and gene expression of matured astrocytes [21–23]. As a result, serum-free procedures for inducing astrocytes have been developed [24, 25]. To accelerate the glial switch in the absence of bovine serum, cells are exposed to epidermal growth factor (EGF) and leukemia inhibitory factor (LIF), which activate the JAK/STAT pathway, while EGF acts as an inhibitor of premature differentiation of NPCs into neurons [26]. Both methods converge during the astrocyte maturation phase, which is facilitated by the presence of CNTF [20, 23].

Previous studies have shown that differentiation protocols for the generation of hiPSC-derived astrocytes vary in terms of reproducibility, maturation stage, and the resulting astrocytes' functionality and phenotype [20, 23, 27, 28]. This study aimed to compare protocols for the differentiation of astrocytes from hi-PSCs that differ in the timing, basic steps, and media used for astroglial progenitor cell induction and astrocyte maturation. We compared two slightly modified versions of the recently introduced protocol established by Perriot et al. [23], which uses a serum-free medium, with the rapid and robust differentiation protocol of Szeky et al. [29]. Both protocols are based on neural stem cells (NSCs) generated by the dual-SMAD inhibition method [30], followed by initiating astrocyte differentiation. Maturation status and activation state of the astrocytes were investigated by using RNA-seq and metabolomic analysis.

Methods

Cell line description

The non-diseased human iPSC line (BIOT.009) used in this study is derived from a healthy female donor and has been previously characterized [31, 32]. Neural stem cells (NSCs) were generated from the iPSCs by dual inhibition of the SMAD signaling pathway using LDN193189 and SB431542 [20], then subsequently used for astrocyte differentiation. SMAD inhibitors were added during the first 21 days of neural induction and FGF was used for both the induction and expansion of the NSCs.

Differentiation of iPSCs-derived NPCs to astrocytes

NPC expansion

NPCs were thawed in completed neural maintenance medium (NMM) (containing 50% DMEM/F12 with glutamine, 50% Neurobasal medium, 1X B27 supplement, 1X N2 supplement, 1% Penicillin/Streptomycin, 1% GlutaMax (all purchased from Gibco), non-essential amino-acids (Sigma), completed with 10 ng/mL recombinant human epidermal growth factor, and 10 ng/mL basic fibroblast growth factor) supplemented with Rhock-inhibitor at a final concentration of 10 µM and plated into poly-L-ornithine/laminin-coated dishes. On the next day, the medium was changed to completed NMM. The cell culture medium was changed every two days. Thawed NPC lines were propagated for the next passage (with a density of 100.000 cells/cm^2) and seeded into Matrigel-coated dishes for astrocyte differentiation at day 10, upon reaching confluence again, (with a cell-density of 50.000/cm^2).

LSFP method of Astrocyte differentiation

We used the modified version of the method published by Silvain Perriot [23] utilizing the glial progenitor cells (GPCs) expansion step described by [33]. NPCs at day 10 were seeded into poly-L-ornithine/laminin-coated plates at a density of 50.000 cells/cm^2 and maintained in GPC expansion medium (containing DMEM/F12 Glutamax, 1X B27-A supplement, 1X N2 supplement completed with 10 ng/ml recombinant human EGF and 10 ng/ml basic fibroblast growth factor (FGF2)) for 2 weeks. The medium was changed every two days. At day 24, cells were seeded into Matrigel-coated plates at a density of 50.000 cells/cm^2 and maintained in astrocyte induction medium (containing DMEM/F12 Glutamax with 1X B27-A supplement, 1X N2 supplement completed with 10 ng/ml recombinant human EGF, and 10 ng/ml LIF) for 2 weeks. The medium was changed every two days. At day 36, cells were plated into Matrigel (50.000 cells/cm^2) in astrocyte maturation medium, which was DMEM/F12 Glutamax medium containing 1X B27-A supplement, 1X N2 supplement, and 20 ng/ml recombinant CNTF (PeproTech, UK). Cells were kept in maturation medium for 4 more weeks with medium changes every two days and cultures were inspected by light microscopic imaging.

SSFP method of Astrocyte differentiation

We used the modified version of the method published by Silvain Perriot [24]. NPCs at day 10 were seeded into Matrigel-coated plates at a density of 50.000 cells/cm^2 and maintained in astrocyte induction medium (containing DMEM/F12 Glutamax with 1X B27-A supplement, 1X N2 supplement completed with 10 ng/ml recombinant human EGF, and 10 ng/ml LIF) for 2 weeks. Medium was changed every two days. When the culture reached confluence, cells were passaged using Accutase for cell-dissociation and seeded into Matrigel-coated 6-well plates with 50.000 cells/cm^2. At day 24, cells

were plated into Matrigel (50.000 cells/cm^2) in astrocyte maturation medium, which was DMEM/F12 Glutamax medium containing 1X B27-A supplement, 1X N2 supplement and 20 ng/ml recombinant CNTF (PeproTech, UK). Cells were kept in maturation medium for 4 more weeks with medium changes every two days and cultures were inspected by light microscopic imaging.

TUSP method of Astrocyte differentiation and treatment

We used our previously described method of Szeky et al. (2024) [29]. Briefly, the NPCs at day 10 were seeded into Matrigel-coated plates at a density of 50.000 cells/cm^2 and maintained in the astrocyte induction medium (ScienceCell's astrocyte growth medium supplemented with 2% FBS) for 4 weeks. The medium was changed every two days. When the culture reached confluence, cells were passaged using Accutase for cell dissociation and seeded into Matrigel-coated 6-well plates with 50.000 cells/cm^2. At day 42, cells were plated into Matrigel (50.000 cells/cm^2) in astrocyte maturation medium, which was serum-free astrocyte growth medium containing 20 ng/ml recombinant human CNTF (PeproTech, UK). Cells were kept in maturation medium for 4 more weeks with medium changes every two days and cultures were inspected by light microscopic imaging.

On day 70 after the end of maturation phase the cells were treated in triplicates with 500 nM Aβ42 (Biotalentum, HU) or 150 uM H_2O_2 for 2 h. Cellular pellets for RNAseq and cellular media for IL-6 analysis were collected 72 h after the treatment.

Analysis of IL-6

The concentration of IL-6 was determined from 105 µl of collected media samples by Interleukin-6 (IL-6) ACCES Immunoassay kit (A16369, Beckman Coulter, USA) on DxI Access Immunoassay Analyzer (Beckman Coulter, USA) according to Instructions.

RNA-Seq experiment

The cellular pellet samples were used to isolate total RNA with TRI Reagent (Merck, USA) and RapidOutput DNA removal kit (ThermoFisher Scientific, USA). A Qubit 4 fluorometer (ThermoFisher Scientific, USA) and Fragment Analyzer (Agilent, USA) were used to analyse the isolated RNA for quantity and quality, respectively. Complementary DNA (cDNA) libraries were synthesized using the NEBNext® Poly(A) mRNA Magnetic Isolation Module and NEBNext® Ultra™ II RNA Library Prep Kit for Illumina® (NEB, UK). The concentration and quality of cDNA libraries were assessed using a Qubit 4 fluorometer (ThermoFisher Scientific, USA) and Fragment Analyzer (Agilent, USA). The cDNA samples were then diluted to 4 nM and sequenced on the Illumina NextSeq® platform with NextSeq® 500/550 High Output Kit v2.5 (150 cycles) (Illumina, USA), generating 75 bp pair-end reads, and on the Illumina NovaSeq® 6000 platform with NovaSeq® S4 300 kit (Illumina, USA), generating 150 bp pair-end reads. The sequencing data, along with the corresponding metadata, are available in the NCBI Gene Expression Omnibus (GEO) repository under the accession number GSE269743.

Sequencing analysis

Data processing was performed as described previously [34]. Briefly, raw sequencing reads were quality-checked using FastQC [35] and were subsequently trimmed using Trim Galore [36]. Following this, the reads were aligned to the human genome sequence hg38, employing the R packages Rbowtie2 [37] and Rsamtools [38]. Differential analysis of count data was performed using the R package DeSeq2 [39]. Transcripts exhibiting $|\log2 \text{ fold change}| > 1$ and $q < 0.01$ (FDR-adjusted P-values) were identified as differentially expressed genes (DEGs). Cluster analysis was conducted using the R packages pvclust [40] and dendextend [41]. To determine the cell type, the R package clustifyr [42] was employed against the scRNA-seq human cortex database [43]. Cellular deconvolution was carried out using BrainDeconvShiny [44] with the assistance of dtangle [45] and the NG database [46]. Heatmaps were constructed using R package ComplexHeatmap [47].

Immunocytochemistry

25–75.000 astrocytes/cm^2 were plated into Matrigel-coated 24-well plates, (containing glass coverslips). On the next day, the cells were fixed with 4% paraformaldehyde, which was followed by permeabilization by 0.2% Triton X-100. Samples were blocked by 3% BSA for 1 h and incubated with the primary antibodies indicated in S1 Table for overnight. Next day, the samples were washed with phosphate-buffered saline (PBS), then incubated with secondary antibodies goat anti-chicken Alexa-488 (#A11039) and donkey anti-mouse Alexa-647 (#A31571), (all purchased from Invitrogen). Nuclei were stained by DAPI. We used Apotome 2 microscope (Zeiss, DE) for fluorescence microscopy imaging.

AMK Analysis

The AMK analysis was performed as previously described in [48]. Briefly, the cultivation medium samples were thawed and mixed with acetonitrile (ACN) to precipitate the proteins. Then, the samples were derivatized with 8.33 mM NaCN, reaction buffer, and 4 µM nVal (internal standard). The analysis was performed on the Agilent G7100A CE System (Agilent Technologies, Germany) coupled with external collinear LEDIF detector

ZETALIF™ LED 480 (Picometrics, France) using an excitation wavelength of 488 nm and emission 515 nm long-pass filter. The derivatized samples were injected into the capillary with a pressure of 50 mbar for 3 s.

Results

Over the past decade, it has become evident that astrocytes play a complex role in the pathology of neurodegenerative diseases, including AD [1, 2]. To investigate the involvement of astrocytes in pathological mechanisms, disease modelling using iPSC-derived cultures has become a popular approach due to the limitations of current animal models. However, the remarkable heterogeneity and plasticity of astrocytes have made it challenging to develop an optimized, short, and cost-effective protocol for producing astrocyte cells in monoculture in vitro [19]. Several protocols have been published in recent decades with the aim of inducing a homogeneous population of functional matured astrocytes in the shortest possible time for the study of AD [18, 20, 24, 27, 33, 49]. However, it remains unclear which protocol is most suitable for the research question. To answer this question, we compared two previously published protocols for generating hiPSC-astrocyte populations that display a phenotype and functions similar to those of human primary astrocytes. We used a validated hiPSC-derived neural progenitor line BIOT.009 negative for the APOE4 allele and did not carrying any chromosomal aberrations or known mutations associated with familial AD. The first 8-week protocol, termed the 'Long Serum-Free Protocol' (LSFP), is based on the method of Perriot et al. [23]. The medium does not contain FBS (as shown in Fig. 1) because its presence can alter astrocyte gene expression, leading to a reactive astrocyte phenotype that

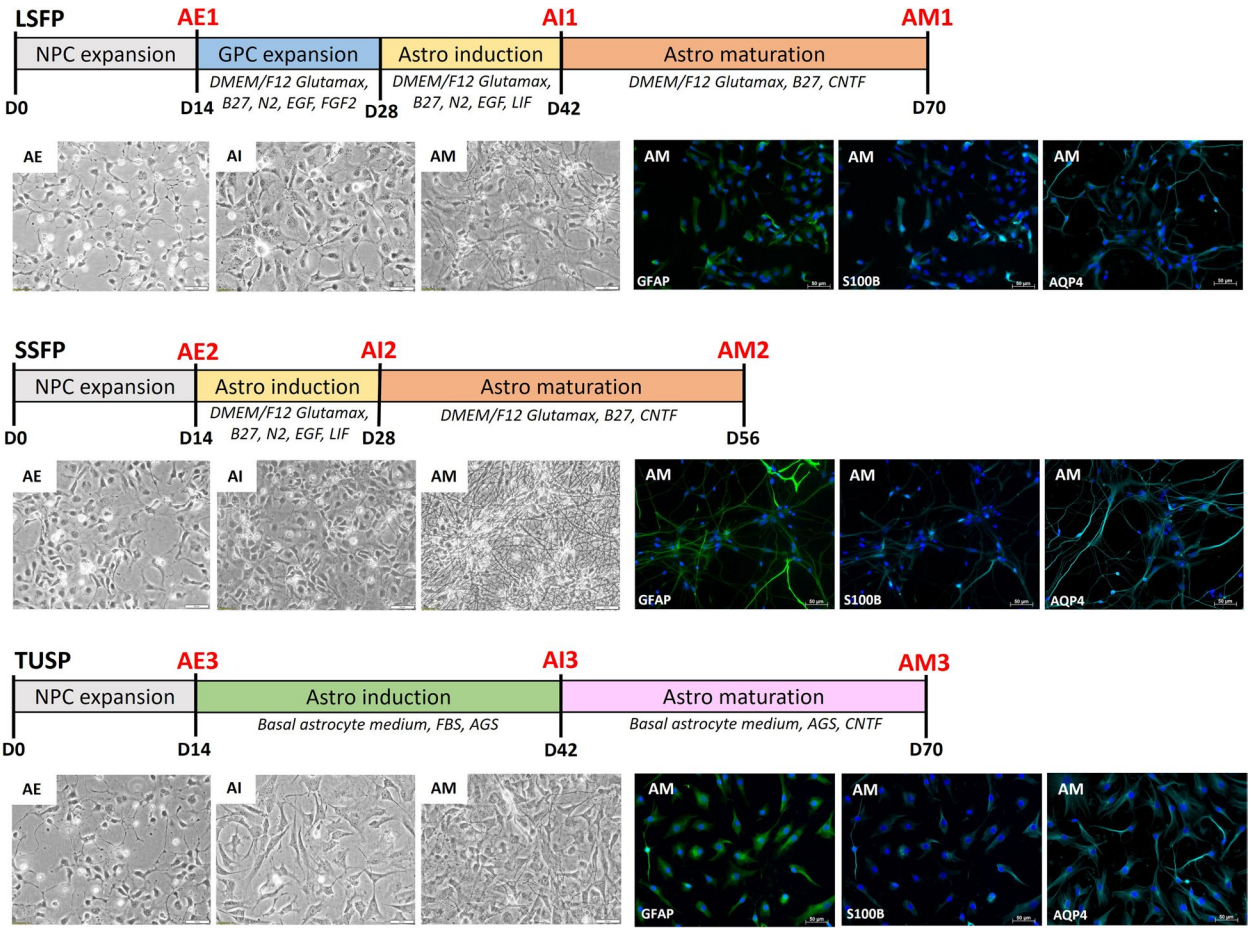

Fig. 1 The differentiation of the astrocytic cultures in this study. Overview of the three used protocols based on medium comprised of DMEM-F12 neurobasal medium and supplements media without FBS (LSFP and SSFP) and commercially available basal astrocytes medium (ScienCell) with the addition of FBS during the induction phase (TUSP). Representative bright-field images and immunofluorescence staining images of hiPSC-derived astrocytes expressing GFAP (Green), S100β (blue), and AQP4 (light blue). Scale bars, 50 µm. Pictures were acquired with a Zeiss Apotome 2 microscope. AGS, Astrocyte Growth Supplement (ScienCell); CNTF, Ciliary Neurotrophic Factor; EGF, Epidermal Growth Factor; FGF2, basic fibroblast growth factor 2; LIF, leukemia inhibitory factor; FBS, fetal bovine serum; NPCs, neural precursor cells

is unsuitable for use as a disease model [22]. The GPCs are expanded for two weeks in the presence of FGF2 and EGF to generate a population suitable for cryopreservation. Following this, astroglia differentiation is induced by exposing the GPCs to leukemia inhibitory factor (LIF) and EGF for two weeks, which activates the JAK-STAT pathway [26]. Over a 4-week period, immature astroglial cells lost their proliferative capacity and acquired specific astrocyte markers using ciliary neurotrophic factor (CNTF) [50]. The second 6-week differentiation protocol, referred to as the 'Short Serum-Free Protocol' (SSFP), is a slightly modified version of the previous protocol by Perriot et al. [23] (Fig. 1), where the step of expanding the glial progenitor cell (GPC) population is omitted. The protocol referred to as the 'Temporary Using Serum Protocol' (TUSP) involves an 8-week differentiation process using commercially available media containing FBS, as described by Tcw et al. [20]. However, FBS is only used for the first 4 weeks, resulting in replicating astrocytes, followed by a further 4 weeks of maturation in the presence of ciliary neurotrophic factor (CNTF) instead of FBS, as described by Szeky et al. (2024) [29] (Fig. 1).

The Generated Astrocytes Resemble Mature Astrocytes

At the start of each protocol, we validated the NPC rosettes and spindle-shaped morphology, as shown in Fig. 1B. During the GPC enrichment phase of the LSFP method, the cells acquired a more triangular morphology typical of astroglia progenitors. The number of neuronal rosettes decreased, but floating cells remained in the culture and were highly proliferative. After the induction of astrocytes, cell proliferation decreased and the cells acquired a triangular shape, the formation of rosettes and the number of floating cells also decreased. Elongated fibers, characteristic of fibrous astrocytes, appeared in the culture after EGF was withdrawn and CNTF was added. The rate of cell proliferation decreased further with maturation (Fig. 1B). In the SSFP method, NPCs were directly induced to differentiate into astrocytes, resulting in the earlier appearance of long fibers. Although the morphology of the cells appeared atypical and the fibers were long and branched, resembling terminal neuronal differentiation, the shape, and orientation of the cell bodies differed from those in a neuronal culture (Fig. 1B). There was a rapid change in cell morphology when astrocytes were induced in commercial media containing FBS in TUSP method. The cells developed triangular bodies shortly after differentiation and maintained this morphology throughout astrocyte induction. When FBS was removed and CNTF was added, the cell bodies became polygonal, and their processes showed different shapes (Fig. 1B). The maturated astrocytes from all three protocols were positive for classical astrocyte markers GFAP, S100β and AQP4, as shown by immunocytochemistry ICC (Fig. 1). Both S100β and AQP4 showed cytoplasmic staining, which were not overlapping with the GFAP staining.The calcium-binding protein S100β was located diffusely in the cytoplasm and around the nuclei of the cells, as it was reported for glial lineage cells [51, 52]. Thus, the molecular phenotype of the cells suggests the morphological and functional characteristics of mature astrocytes.

Induction Time is Critical for the Proper Maturation of Astrocytes

An RNA-seq experiment was done to investigate the differences between astrocytes produced by different protocols. When comparing the global gene expression pattern across our protocols and other astrocyte studies, the principal component analysis only revealed a distinctive divergence in TUSP method, resembling the fetal astrocytic transcriptomic pattern from the study of Crowe et al. [53] (Fig. 2A). Next, a pair-wise differential expression analysis of abundant transcripts was done after the maturation phase of astrocyte differentiation using the original studies (fold change > 2, base mean > Q3, adjusted $p < 0.01$). As the astrocytes in TUSP method after the 4-week induction phase represent the previously published study of TCW et al. [20], we also include this comparison in the analysis.

In general, TUSP method showed the least differences, while SSFP method showed the greatest differences when comparing the overall pair-wise gene expression between our astrocyte cultures and the original studies (Fig. 2B). After examining the changes in the DEG profile, we investigated in detail the specific differentially expressed genes (DEGs, fold change > 2, base mean > Q3, adjusted $p < 0.01$) in the three protocols following the induction and maturation phases. Due to the use of the same basal medium and supplements for induction, the lack of DEGs between LSFP protocol and SSFP protocol after the astrocyte induction phase (Fig. 2C) is not so surprising, despite the additional GPC expansion step in LSFP method (Fig. 1A). However, after the maturation phase, there were 476 DEGs comparing LSFP and SSFP methods. Among the upregulated genes in SSFP astrocytes, we identified an enrichment of several pathways involved in NGF-stimulated transcription, RNA processing, translation initiation, or Rho GTPase signaling that regulates cytoskeletal dynamics (Fig. 3A, B, D). This could indicate a proliferative status of these cells with a low degree of maturation, corresponding to the observed differences in cell morphology (Fig. 1B).

The analysis of amino acids in media from astrocytes differentiated according to LSFP and SSFP protocols revealed no significant differences after the induction phase (Fig. 3). The cells' proliferative status was indicated

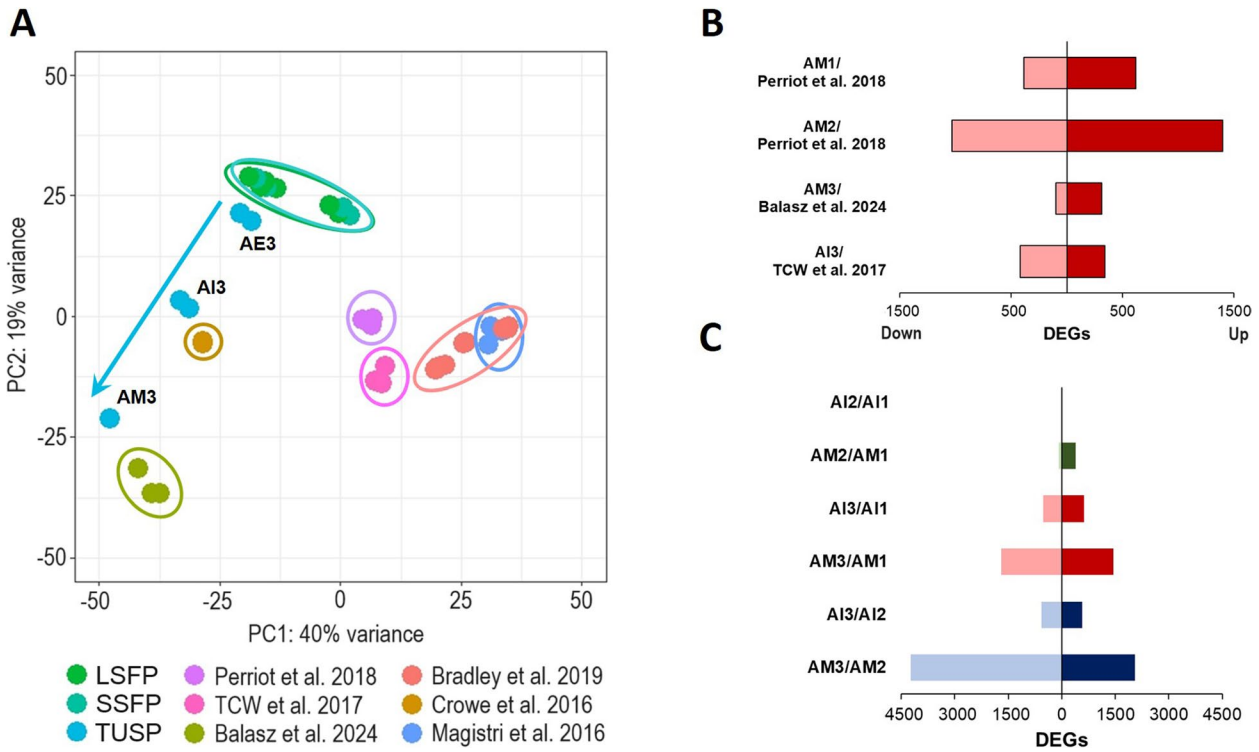

Fig. 2 Changes in global expression patterns. **A** Principal component analysis of 3 differentiation protocols (LSFP, SSFP, and TUSP) together with original protocols from publications (Perriot et al. [23], Balazs et al. 2024 and TCW et al. [20]), fetal astrocyte culture (Crowe et al. [53]), and astrocytes differentiated from hNPCs (Magistri et al., [22]) and hPSCs (Bradley et al., [54]). The blue line indicates the differentiation trajectory (AE-end of expansion, AI-end of induction, AM-end of maturation). **B**, **C** Differentially expressed genes (DEGs) (fold change > 2, base mean > Q3, adjusted $p < 0.01$) among three used protocols (AX1-3) in the pair-wise comparisons with original studies (**B**) and differentiated phases (**C**). AI – end of induction, AM – end of maturation)

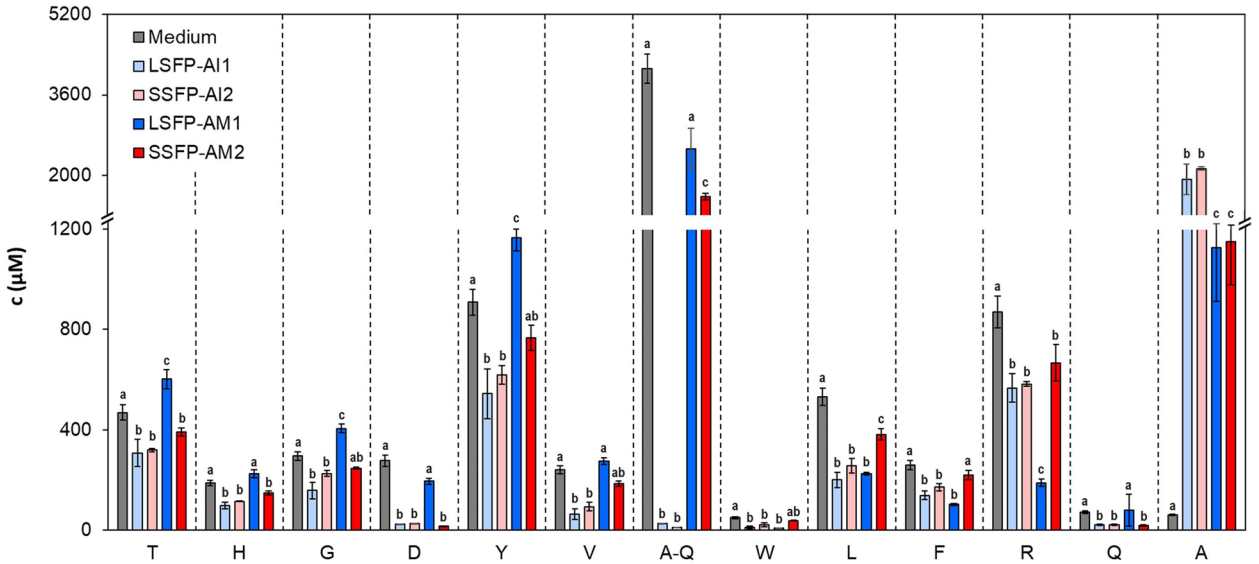

Fig. 3 Differences in amino acids levels. Bar chart showing metabolic turnover of selected AAs and GlutaMax (AQ) in the medium of cultivated astrocytes at the end of induction (AI) and maturation (AM) phases of LSFP and SSFP methods. The media were collected 3 days after the passage of the cells ($n = 3$). The error bars represent standard error. Different letters show levels of statistical significance analyzed by Student's t-test: * $P < 0.05$

by their high consumption rate of GlutaMax, a dipeptide hydrolyzed by aminopeptidases to L-glutamine (Fig. 3). L-glutamine is an essential amino acid that provides carbon and nitrogen to fuel biosynthetic processes during cell proliferation [55]. The proliferative status of astrocyte progenitor cells is indicated by the consumption of amino acids such as L-aspartate, which serves as a precursor for nucleotide synthesis and plays a critical role in redox balance through the malate-aspartate shuttle [56]. Additionally, L-arginine accumulates in astroglial cells, and branched-chain amino acids (BCAAs) (leucine and valine) act as major nitrogen donors [57] (Fig. 3). After the maturation phase, the consumption rate of many of these amino acids decreased significantly in the LSFP method, with only high accumulation of L-arginine. However, in the SSFP method, there was a sustained higher amino acid consumption, confirming the RNAseq results showing a proliferative state with a low degree of maturation (Fig. 3).

Presence of FBS Induces Major Changes in the Extracellular Matrix Organization

Analysis of TUSP method revealed the identification of 1140 DEGs compared to LSFP and SSFP protocols after induction (Fig. 2C), demonstrating the effect of the different mediums used together with the addition of FBS play a significant role in supporting cell growth and proliferation and the synthesis of extracellular matrix (ECM) components in cell culture [58]. The growth factors present in FBS, such as FGF, insulin-like growth factors (IGFs), and transforming growth factors (TGFs), induce observed upregulation of PI3K/AKT, mitogen-activated protein kinase (MAPK), canonical Wnt and transforming growth factor-beta (TGF-β) signaling pathways (Fig. 4C) essential for maintaining the stemness of human PSCs [59, 60]. The observed upregulation of the pathway to ECM organization (Fig. 4C, D) corresponds to the fact that FBS contains an array of growth factors and cytokines that stimulate cells to produce ECM components, provide cell adhesion molecules such as fibronectin and vitronectin that facilitate adhesion to the culture substrate and plays a critical role in regulating ECM synthesis via signaling pathways [61]. Indeed, the morphology of the actin cytoskeleton is influenced by FBS [62] as observed here in the upregulation of genes connected to the Rho-GTPase signaling pathway involved in the reorganization of the actin cytoskeleton like filopodia formation involving the small up-regulated GTPase Rif (RhoF) [63] (Fig. 4D). The reorganization of the cytoskeleton is also connected with the shape of the cells when astrocytes having polygonal shapes, as observed here, exhibit actin fibers and conversely, those with stellate shapes lack them [64] (Fig. 1b).

A more profound disparity was observed after the maturation phase, with 3141 DEGs and 6280 DEGs being identified in LSFP and SSFP protocols, respectively (Fig. 2C; Fig. 5). Most genes that were upregulated participated in the ECM organization process (Fig. 4C, D; Fig. 5). This is consistent with the notion that the maturation of astrocytes is accompanied by changes in the expression of a wide range of ECM proteins [65], and astrocytes possess a crucial function in the production of ECM molecules [66]. We observed higher expression levels of glycoproteins fibrillins, laminins, and nidogens in addition to collagen in the brain's extracellular matrix (Fig. 4D). Consistent with changes in ECM molecules, there was an increase in the expression of matrix metalloproteinases (MMPs) MMP2, MMP14, and MMP23A, which cleave ECM proteins including brevican, tenascin, aggrecan, laminin and collagens (Fig. 4D). Activation of these proteins is critical for normal physiological function but is also implicated in the regulation of many pathological processes [67]. Furthermore, we observed an increase in the expression of disintegrin and metalloproteinase enzymes containing thrombospondin motifs (ADAMs and ADAMTSs, respectively) involved in the regulation of the extracellular matrix composition and MMP activity (Fig. 4D). Notably, the upregulated ADAMTS-5 showed specificity for targeting chondroitin sulfate proteoglycans (CSPGs) that are abundantly produced by reactive astrocytes [67], and whose metabolism was downregulated (Fig. 4D). The observed downregulation of pathways related to the neuronal system and nervous shows a successful astrocyte maturation process (Fig. 4C).

Mature Astrocytes Derived from hiPSCs Exhibit a More Fetal-like Astrocyte Profile

To characterize the level of maturation of the differentiated astrocytes and their similarity to primary astrocytes, we assessed the expression of 46 genes enriched in a given cell type (Fig. 6A). Human iPSC-derived astrocytes induced by all three protocols displayed a pattern similar to human primary astrocytes, with enrichment in astrocytic markers. Noticeably, astrocytes differentiated by LSFP and SSFP protocols showed increased levels of some neuronal cell marker genes, and astrocytes differentiated by TUSP protocol showed a high expression of gene coding transmembrane protein 119 (TMEM119). To further characterize the astrocyte cultures, we used bulk RNA-seq platforms with the 'dtangle' deconvolution method [45]. Cell type proportions were estimated in our astrocyte culture alongside fetal and primary astrocytes from previous studies [25, 53], as well as hiPSCs [20, 23], hNPCs [22], and hPSCs [54] using publicly available prefrontal

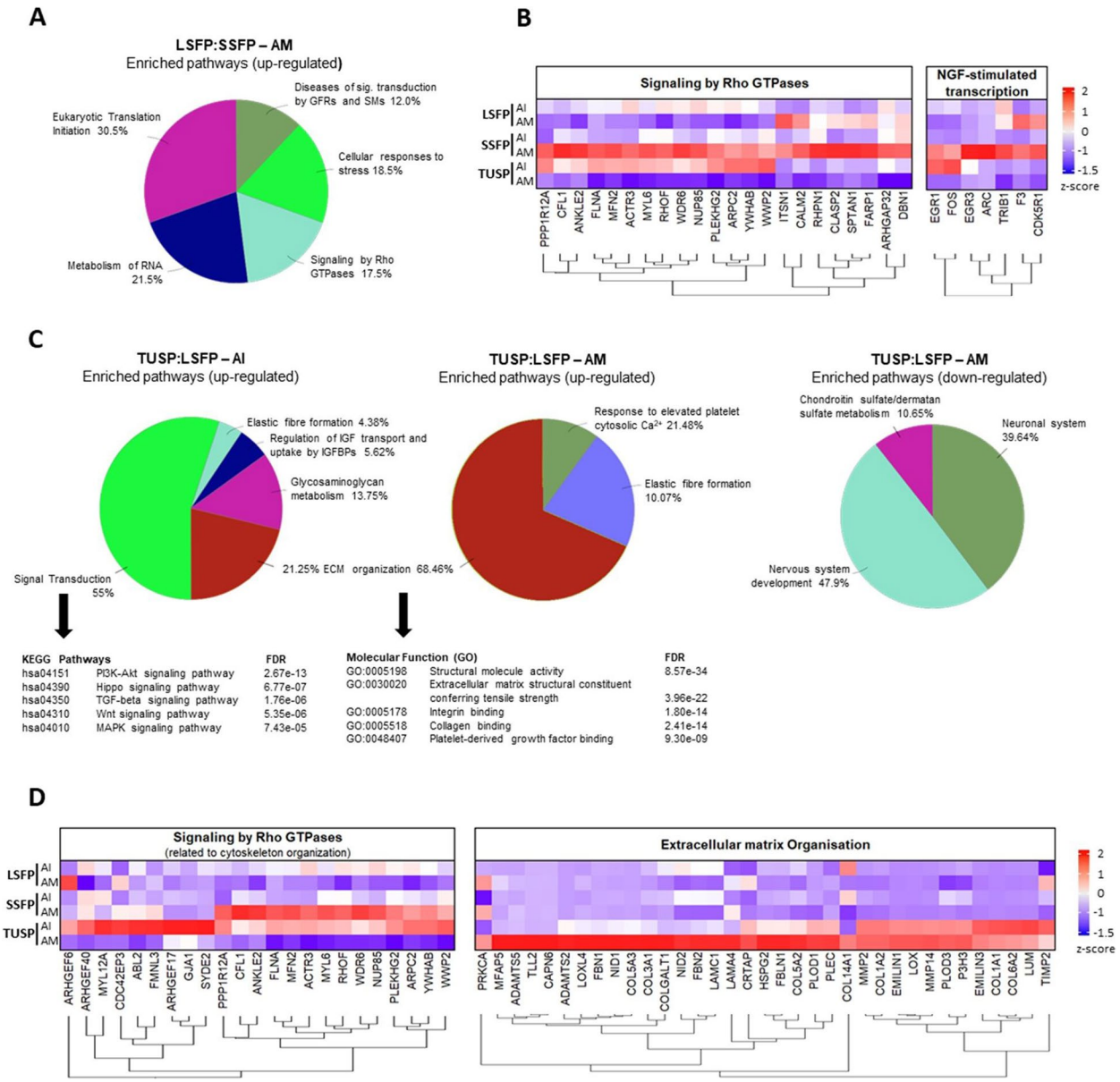

Fig. 4 Transcriptomic changes during differentiation of iPSC into mature astrocytes. **A** Reactome pathway term enrichment analyses were performed for up-regulated genes and down-regulated genes between LSFP and SSFP methods after maturation phase (fold change > 2, base mean > Q3, adjusted $p < 0.01$). **C** Reactome pathway term enrichment analyses were also performed for up-regulated genes and down-regulated genes between TUSP and LSFP methods after induction or maturation phase. The same criteria were used for gene selection and statistical significance. **B**, **D** The heatmap shows the basemean expression profile of genes in enriched Reactome pathways (FDR < 0.01) for LSFP and AAFP methods (B) and TUSP and LSFP methods (D) after induction (AI) or maturation (AM) phase

cortex single-nucleus transcriptomic data [46]. Notably, except for primary astrocytes, we were unable to identify a cell culture with a gene expression profile matching that of mature astrocytes from the scRNA-seq study of the prefrontal cortex (Fig. 6B). Astrocytes differentiated using LSFP and SSFP protocols exhibited a combination of neurons and astrocytes, with a higher proportion of neurons similar to that observed in the study by Magistri et al. [22]. The cells differentiated using the TUSP method exhibited an even distribution of neurons, astrocytes, and OPCs, closely resembling the methods utilized by Perriot et al. [23], TCW et al. [20], and fetal astrocytes (Fig. 6B).

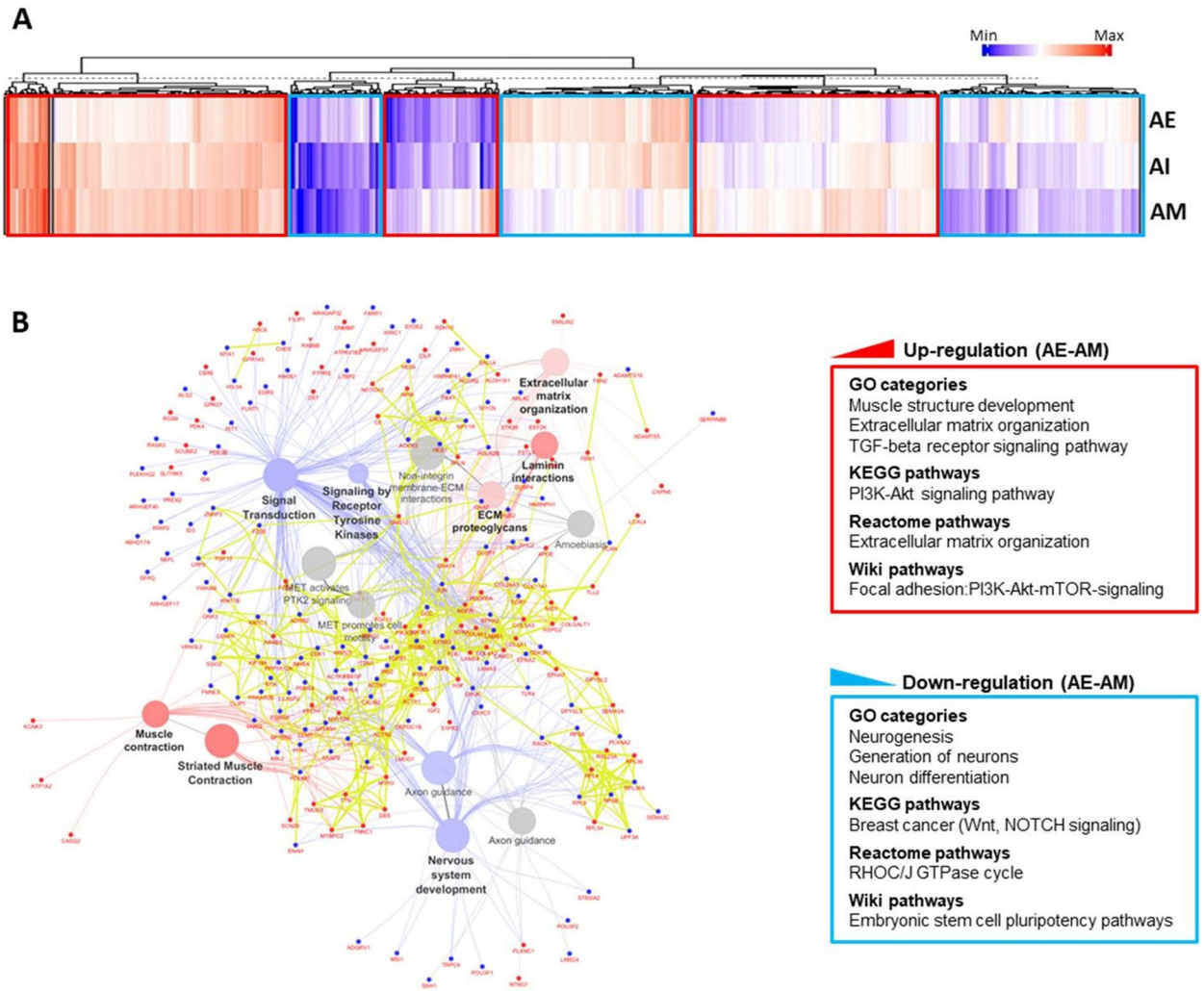

Fig. 5 The transcriptome undergoes reprogramming during astrocyte differentiation in the TUSP method using FBS. **A** The RNA-seq data is presented in a hierarchical clustering and heat map format, displaying all differentially expressed genes between AE-AM samples. The DEGs were divided into two clusters based on their expression patterns. The associated GO categories, KEGG, Reactome and Wiki pathways for each cluster are shown below the heat map. **B** The ClueGo Cytoscape plug-in was used to perform KEGG and Reactome pathway analysis. A list of unique genes was generated from statistically significant regulated transcripts (> twofold change and Padj < 0.05) among AM3 and AI3 transcript levels. Lists of down-regulated (blue) and up-regulated (red) transcripts were used to query the KEGG and Reactome pathways. The ClueGo parameters were set as follows: Go Term Fusion was selected, only pathways with P-values < 0.01 were displayed, and a kappa score of 0.40 was used

A Reactive Astrocyte Phenotype is not Induced by the Temporary Presence of FBS

As FBS has been shown to induce a reactive phenotype in culture [22, 23, 25], we conducted additional analysis of the expression of several genes previously associated with this phenomenon in hiPSC-derived astrocytes from TUSP method, cultured with FBS during the induction phase. Magistri and colleagues (2016) used gene set enrichment analysis to identify a set of marker genes that were upregulated in astrocytes derived from NPC in response to FBS exposure [22]. Only seven of these marker genes were strongly upregulated during the induction phase in the presence of FBS (see Fig. 6C). In contrast, during the subsequent maturation phase without FBS and in the presence of CNTF, the expression of all these genes decreased, while the expression of another set of six genes increased (see Fig. 6C). No effect of FBS on GFAP expression was observed (Fig. 6C), which is a hallmark of reactive astrocytes characterized by upregulation, increased secretion of CSPGs [68], and expression of immature markers such as NESTIN [69] and VIMENTIN (VIM) [70]. Notably, after the maturation phase in TUSP method, a decrease in the expression level of

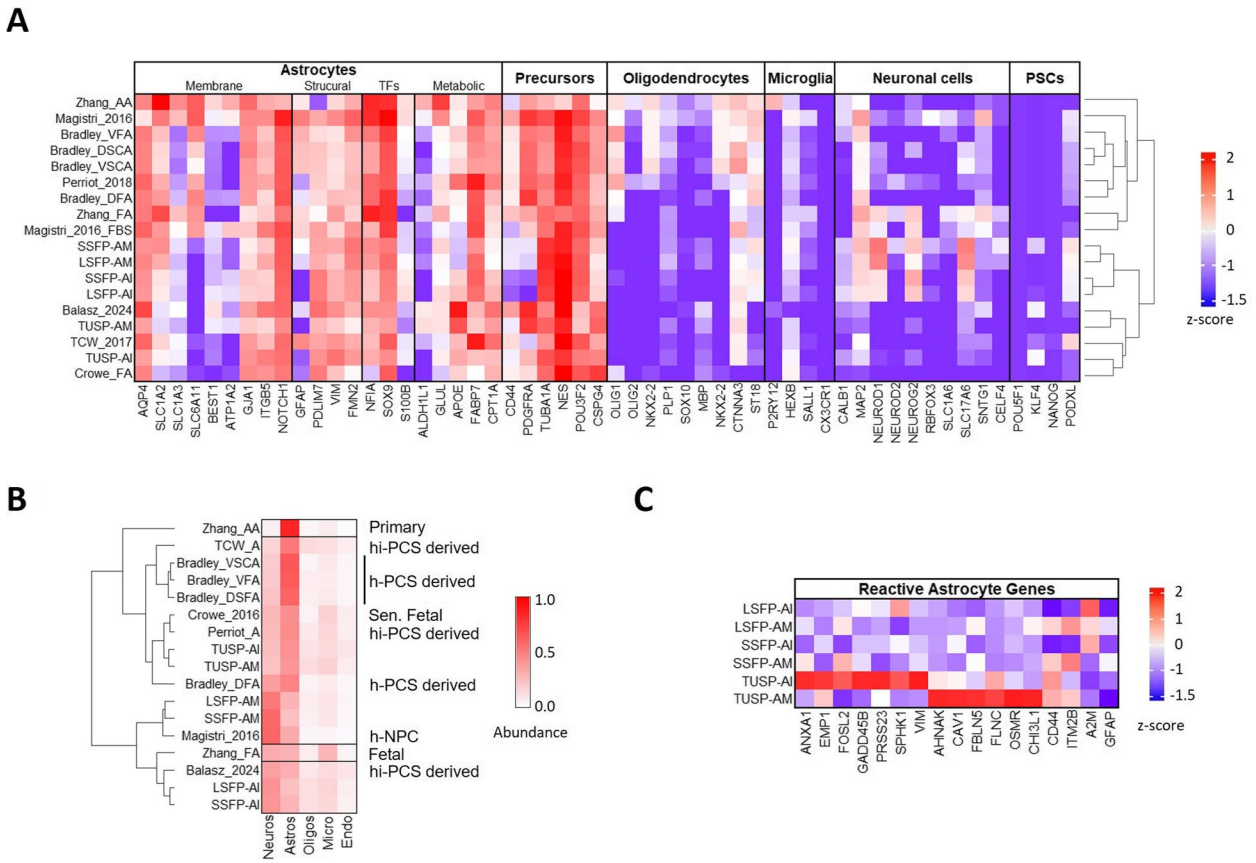

Fig. 6 The level of maturation of the differentiated astrocytes from iPSCs. **A** Heatmap showing basemean expression profile of the 54 marker genes from hiPSC-derived astrocytes, primary astrocytes (Zhang_AA [25]), hiPSCs derived astrocytes (TCW_A [20], Perriot_A [23]), hPSC-derived astrocytes (Bradley [54]), NPC-derived astrocytes (Magistri_A [22]) and fetal astrocytes (Zhang_FA [25], Crowe_FA [53]). **B** Heatmap showing the percentage of generated astrocytic cultures sharing the expression signatures with the prefrontal cortex single-nucleus transcriptomic data [46]. **C** Heatmap showing basemean expression profile of the core genes related to FBS reactive-astrocytes genes signature according to study of Magistri et al. [22]. A—Astrocytes, AA – Adult Astrocytes, FA – Fetal Astrocytes, VFA—Ventral Forebrain Astrocytes, DFA—Dorsal Forebrain Astrocytes, VSC—Ventral Spinal Cord Astrocytes, DSC—Dorsal Spinal Cord Astrocytes

VIM (Fig. 6C) was observed, as well as a decrease in the CSPGs metabolic pathway (Fig. 6C).

TUSP astrocytes respond to Aβ42 and oxidative stress

To further demonstrate the applicability of TUSP astrocytes for AD research, we treated mature astrocytes with Aβ42 peptide and oxidative stress (represented by hydrogen peroxide H_2O_2). To overcome the toxic effects of μM concentrations of Aβ42, we used a 500 nM concentration of Aβ42, corresponding to synaptotoxic concentrations when brain clearance is impaired [71]. In the case of H_2O_2, cells were treated with 200 μM hydrogen peroxide for 2 h, which has no toxic effect on astrocytes. Analysis of secreted IL-6, a key effector of the astrocyte neuroinflammatory response in neurodegenerative diseases, showed that resting astrocytes secreted low levels of IL-6 (mean = 4.9 pg/ml). Treatment with both Aβ42 and H_2O_2 resulted in an increase in IL-6 secretion (Fig. 7C). To further characterize the response of TUSP astrocytes, we performed RNA sequencing analysis of mature TUSP astrocytes exposed to Aβ42 and H_2O_2. To identify functional categories of differentially expressed transcripts in treated astrocytes, we performed GO enrichment analysis using biological process and functional terms with the functional annotation clustering tool in the Cytoscape plug-in ClueGo [72], using a cut-off of 1.5-fold differential expression ($P_{adj} < 0.05$) to define up- or down-regulated genes. Treatment of cells with H_2O_2 resulted in more than a twofold increase in the number of up-regulated transcripts (Fig. 7) compared to treatment with Aβ42. The processes involved in cell migration were enriched among the upregulated transcripts common to both treatments (Fig. 7). On the other hand, Aβ42 treatment down-regulated transcripts are involved in the process of L13a-dependent translational control, which plays a critical role in delaying inflammation in cells [73, 74].

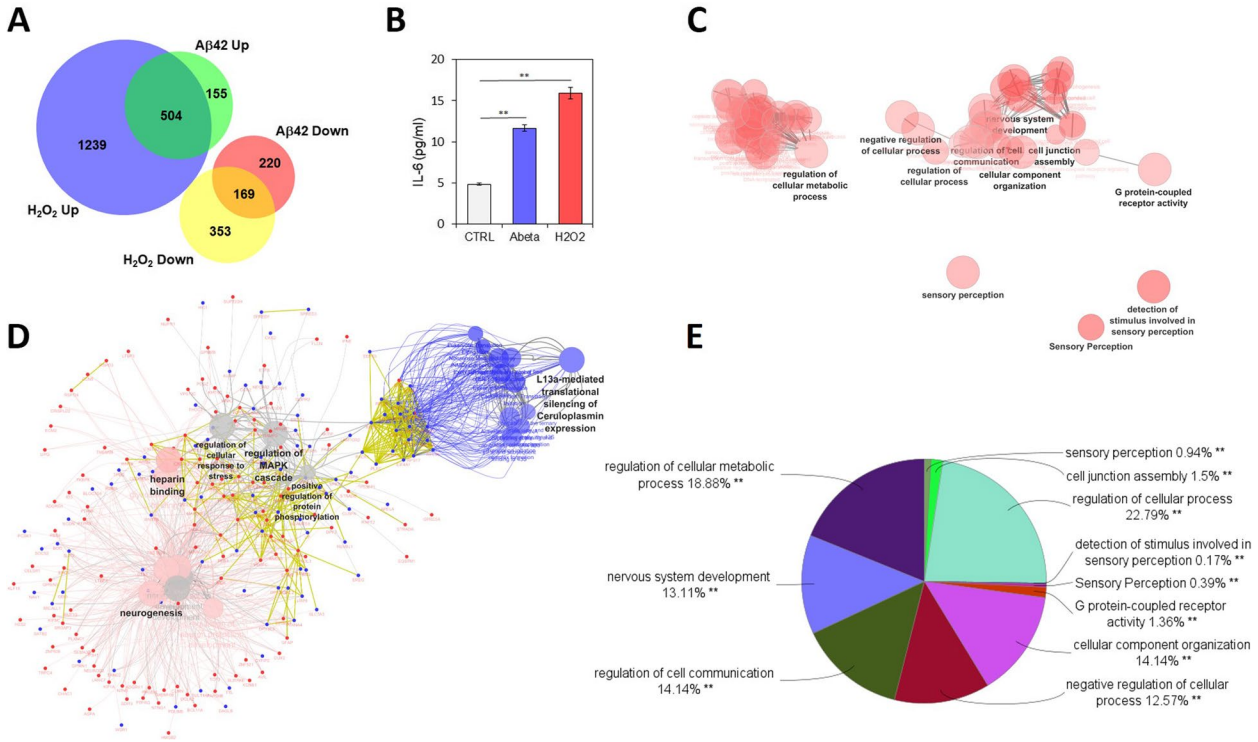

Fig. 7 The response of the TUSP astrocytes to Aβ42 and oxidative stress. **A** The Venn diagram showing intersection between the differently expressed transcripts 72 h after treatment of maturated TUSP astrocytes by 500 nM Aβ42 and 200 µM H_2O_2. **B** The IL-6 levels in media 72 h after treatment of maturated TUSP astrocytes by 500 nM Aβ42 and 200 µM H_2O_2. The error bars represent standard error ($n = 3$), statistical significance was analyzed by Student's t-test, ** $P < 0.01$. **C**, **D**. The ClueGo Cytoscape plug-in was used to perform GO and Reactome pathway analysis. A list of unique genes was generated from statistically significant regulated transcripts (> twofold change and $P_{adj} < 0.01$) 72 h after treatment of maturated TUSP astrocytes by 500 nM Aβ42 (**D**) or 100 µM H_2O_2 (**C**). Lists of down-regulated (blue) and up-regulated (red) transcripts were used to query the GO Biology process and function, and Reactome pathways. The ClueGo parameters were set as follows: Go Term Fusion was selected, only pathways with P-values ≤ 0.01 were displayed, and a kappa score of 0.40 was used. **E** The overrepresented GO biological process classes within astrocyte upregulated transcripts (> twofold change and $P_{adj} < 0.01$) after treatment of maturated TUSP astrocytes by 200 µM H_2O_2

The next large set of up- and downregulated transcripts were involved in processes related to the regulation of the stress response, including the MAPK cascade or protein phosphorylation. The last group of mainly up-regulated transcripts were involved in processes related to the development of the neuronal system after injury or brain diseases (Fig. 7). In the case of H_2O_2 treatment, there was an up-regulation of transcripts related to the processes of signal perception and transduction, regulation of metabolic processes, cell communication or nervous system development and show a high similarity with previously characterized changes in astrocytes within oxidative stress-induced senescence [53].

Discussion

In the past decade, it has become evident that astrocytes play a vital role in synapse formation and function, neurotransmitter release and uptake, neuronal metabolism, and amyloid-beta (Aβ) clearance [2, 75–77]. Therefore, it is crucial to comprehend the astrocyte subtypes related to AD to discover new pathophysiological mechanisms of the disease. Recent advances in iPSC technology have provided groundbreaking opportunities in AD research [78, 79]. Multiple protocols for differentiating iPSCs into astrocytes are available [18, 20, 24, 50, 80, 81], but the research community is continuing to refine these methods to increase the yield, purity, and maturity of cells in the most efficient and cost-effective way possible. The aim of our study was to compare methods that represent two basic methodological approaches. The first approach represents two methods referred to as LSFP and SSFP. These methods are based on chemically defined media and do not use FBS [23, 24] (cited more than 100 times to date). The second approach represents a method referred to as TUSP, based on a method that uses FBS for a limited time during astrocyte induction. This method is based on a straightforward, widely employed method [20] (cited more than 250 times to date). The two approaches differ

in the media used, time of cultivation, and mainly the presence of FBS during astrocyte induction. This raises questions about their applicability to different scientific tasks. Therefore, we performed a comprehensive transcriptomic analysis and compared it with previous RNAseq studies included astrocyte cultures derived from hPSCs [54], NPCs [22], fetal tissue [53] and primary astrocytes [25].

The use of serum for the differentiation of astrocyte cultures is a controversial issue. Although most serum proteins are unable to cross the blood–brain barrier, astrocytes are in contact with blood vessels *in-vivo*, and serum may contain unknown signals that are necessary for astrocyte differentiation. Some authors have opposed the use of FBS in astrocyte differentiation due to concerns about batch inconsistencies and the unknown amount of growth factors and hormones, which may lead to lower experimental reproducibility. However, studies conducted on astrocyte differentiation prior to the expansion of the iPSC method provide evidence that differentiation under serum-containing conditions favors the generation of astrocytes over neurons and reduces the presence of neuronal cells. This approach is beneficial when aiming to establish a purely astrocytic model through cultivation. Studies have described a reduction in the number of neurons in culture and a preference for differentiation into astrocytes in the presence of serum when investigating the effect of FBS on the differentiation of various cell types, including those derived from hiPSCs, mouse spinal cord astrocytes [82], human pluripotent stem cells [50], rat-derived hippocampal neurons [83], and neural stem/progenitor cells isolated from rat embryos [84, 85] and human iPSC lines [28]. Our findings support this phenomenon as certain neuronal markers showed an increase, indicating possible contamination with neurons during the later stages of induction and maturation in both FBS-free methods (LSFP and SSFP). However, cells from the TUSP method that were cultured with FBS during the induction phase exhibited reduced expression of all neuronal markers. This was further supported by the deconvolution analysis, which reveals the cell type proportions in cell culture after the maturation phase. The TUSP method shares expression signatures that are more similar to an astrocytic profile, while the LSFP and SSFP methods tend to lean towards a neuronal profile. This supports previous findings that serum has a positive effect on the preferential differentiation of progenitor cells into astrocytes, while minimizing neuron formation [28, 83, 85]. Moreover, the results of our SSFP method suggest that attempting short-term astrocyte differentiation without FBS is unlikely to be successful and FBS is currently the only way to minimize neuron formation during cultivation if a pure astrocyte culture is desired in a short time. This is consistent with the approach of Mulica et al. [28], who used a short-term serum-containing protocol instead of long-term serum-free culture in their research.

Today, there is no dispute that astrocytes differentiated under serum-containing and serum-free conditions significantly differ from each other, both transcriptionally and morphologically which is supported by studies on isolated neuronal cells or iPSCs that were differentiated into astrocytes in the presence or absence of FBS [22, 23, 25, 86]. Our findings are consistent with these reports. However, the differences between the protocol with and without FBS are more noticeable at the end of the maturation phase when FBS is absent from the medium. This demonstrates that the presence of FBS during the induction phase triggers lasting changes in cells that significantly affect overall cellular metabolism, even after its removal from the medium. During the induction phase, the LSFP and TUSP methods exhibited significant differences. In the TUSP method, the cells rapidly transformed into triangular bodies, which could be attributed to the upregulation of genes associated with the Rho-GTPase signaling pathway. These genes are involved in the reorganization of the actin cytoskeleton and cell shape [62, 64]. Furthermore, the activation of the JAK-STAT pathway was observed to accelerate the switch toward glial cell differentiation [26], which supports the positive effect of FBS on short-term astrocyte differentiation.

During the maturation phase of the TUSP method, the removal of FBS from the medium led to a decrease in cell proliferation capacity as expected, due to the presence of growth factors in FBS. However, genes related to extracellular matrix processes were also significantly upregulated, which corresponded with the extensive extracellular matrix formation observed by cells from the TUSP method under microscopy. In the brain, astrocytes produce the ECM which supports axonal outgrowth and neural cell migration, contributing to neural development. Additionally, the maintenance of trisynaptic connections, a crucial element of the hippocampal circuitry involved in memory processing and spatial navigation, requires a complex interplay of signals and structural components, including those provided by astrocyte-derived ECM molecules [65]. The increased expression of glycoproteins, such as fibrillin and laminins, observed in the TUSP protocol is consistent with the well-documented production of these proteins in fetal and primary cultures of human astrocytes from postmortem brain tissue samples [87–89]. Although the observed expression of collagen in the brain's ECM is typically limited, the spinal cord of astrocyte-depleted mice exhibited significantly reduced levels of basement-membrane-associated ECM molecules, such as laminin and nidogen, as well as

non-basement membrane-associated ECM molecules, such as collagen [66]. Proteoglycans represent the next types of astrocyte-derived matrix molecules essential for the development and maintenance of trisynaptic connections. During development and after a lesion, astrocytes express a wide range of proteoglycans, which contribute significantly to the glial scar. Membrane-associated heparin sulfate proteoglycans (HSPGs) play a crucial role in FGF-2 signaling. They have also been implicated in supporting the signaling of morphogens such as Wnt proteins, which regulate neural stem cell proliferation. In contrast, CSPGs are expressed by reactive astrocytes and are enriched in CNS scar tissue after lesions. They are believed to inhibit axon regeneration. The therapeutic potential of ChABC has been widely discussed in recent years due to its ability to eliminate CSPGs and improve functional recovery in the central nervous system after injury.

It is noteworthy that in our TUSP method using FBS for only a short time during the induction of astroglia, we observed a down-regulation of processes related to the synthesis of CSPGs. This fact, together with the low level of typical marker genes whose expression is associated with reactive astrocytes [76], suggests that the short presence of FBS did not result in a reactive phenotype of astrocytes, which is not suitable for AD research. Although in the TUSP method, we observed increased expression of some genes previously associated with a reactive phenotype [22], these genes in the majority did not represent typical markers of reactive astrocytes, and their expression was repeatedly observed in different subtypes of astrocytes under physiological conditions. Moreover, the study of Tcw et al. [20] using FBS during the whole period of differentiation of hiPSC astrocytes showed their quiescent expression and proved their use in the study of neuropsychiatric disorders [20]. The stimulation of hiPSC-derived astrocytes by the TUSP method with a low non-neurotoxic concentration of Aβ42 peptide, which exceeds the aggregation concentration [90] and oxidative stress, results in increased levels of IL-6 and transcriptomic changes in astrocytes with modulated genes related to the regulation of the stress response, as observed in previous studies [53]. Consequently, the TUSP protocol represents an optimal platform for preliminary disease modeling, given the high degree of maturity of the resulting cells.

Conclusions

In conclusion, we have shown that astrocytes generated by the TUSP method express typical astrocytic markers together with a more intense remodeling of the extracellular matrix compared to the LSFP and SSFP methods. The presence of FBS in the TUSP method increased the purity of the astrocytic culture and eliminated the neuronal phenotype of differentiated astroglia. In addition, the need for a long induction was evident in the FBS-free methods, supporting the use of FBS in the medium for less time-consuming protocols suitable for research. We presented a comprehensive transcriptomic comparison of the protocols, suggesting that FBS does not necessarily have a negative effect on the resulting cells and may be crucial for differentiation under certain conditions. Our findings could provide researchers with relevant information when choosing the optimal protocol for their research questions.

Supplementary Information

The online version contains supplementary material available at https://doi.org/10.1186/s12575-024-00257-y.

Supplementary Material 1.

Authors' contributions

VJ, BS, MZ, AF, JH, RK, SP and JL performed experiments. MZ, MZa, VJ, JL, RK performed the analysis. VJ, MZa, BS, RK, OS, AD and JL wrote the manuscript, which was reviewed by all the authors. BS, AF, MZa contributed to iPSC generation. AD and RK acquired funding for this study and together with JL supervised the work.

Funding

This study was supported by the Ministry of Health, Czech Republic (NU20-09–00437) received by JL and RK, by Hungarian Grants No. 2020–1.1.5-GYORSÍTÓSÁV-2021- 00016 and by the ERA-NET NEURON Research Programme (No. 2019–2.1.7-ERANET-2022–00031, NDCil), received by AD. The funders had no role in study design, data collection and analysis, decision to publish, or preparation of the manuscript.

Availability of data and materials

The sequencing data, along with the corresponding metadata, are available in the NCBI Gene Expression Omnibus (GEO) repository under the accession number GSE269743. Use the following secure token "qzwzmgoalxmtfaf" to review the record GSE269743.

Declarations

Ethic approval and consent to participate

Our research fully adheres to ethical standards and guidelines. The ethical licence was issued by the Scientific and Research Ethics Committee of the Hungarian Health Science Council for "Production of induced pluripotent stem cells (IPS) from human somatic samples" with the following ID No.: IV/3935- 1/2021/EKU in May 2021. The study was conducted according to the guidelines of the Declaration of Helsinki, and approved by the Ethical Committee, University Hospital Pilsen and Faculty of Medicine in Pilsen, Charles University, Edvarda Beneše 1128/13, 30599 Pilsen – Czech Republic (email: etickakomise@302 fnplzen.cz) on 19th June 2019.

Consent for publication

Not applicable.

Competing interests

The authors declare no competing interests.

Received: 28 June 2024 Accepted: 9 September 2024
Published online: 28 September 2024

References

1. Verkhratsky A, Parpura V, Rodriguez-Arellano JJ, Zorec R. Astroglia in Alzheimer's Disease. Adv Exp Med Biol. 2019;1175:273–324.
2. Verkhratsky A, Butt A, Li B, Illes P, Zorec R, Semyanov A, et al. Astrocytes In Human Central Nervous System Diseases: A Frontier For New Therapies. Signal Transduct Target Ther. 2023;8:1–37.
3. Sonninen T-M, Hämäläinen RH, Koskuvi M, Oksanen M, Shakirzyanova A, Wojciechowski S, et al. Metabolic Alterations In Parkinson's Disease Astrocytes. Sci Rep. 2020;10:14474.
4. Tripathi P, Rodriguez-Muela N, Klim JR, de Boer AS, Agrawal S, Sandoe J, et al. Reactive Astrocytes Promote Als-Like Degeneration And Intracellular Protein Aggregation In Human Motor Neurons By Disrupting Autophagy Through Tgf-**B**1. Stem Cell Rep. 2017;9:667–80.
5. Fontana IC, Scarpa M, Malarte M-L, Rocha FM, Ausellé-Bosch S, Bluma M, et al. Astrocyte Signature in Alzheimer's Disease Continuum through a Multi-PET Tracer Imaging Perspective. Cells. 2023;12:1469.
6. Matyash V, Kettenmann H. Heterogeneity In Astrocyte Morphology And Physiology. Brain Res Rev. 2010;63:2–10.
7. Molofsky AV, Deneen B. Astrocyte development: A Guide for the Perplexed. Glia. 2015;63:1320–9.
8. Namihira M, Kohyama J, Semi K, Sanosaka T, Deneen B, Taga T, et al. Committed Neuronal Precursors Confer Astrocytic Potential On Residual Neural Precursor Cells. Dev Cell. 2009;16:245–55.
9. Barnabé-Heider F, Wasylnka JA, Fernandes KJL, Porsche C, Sendtner M, Kaplan DR, et al. Evidence That Embryonic Neurons Regulate The Onset Of Cortical Gliogenesis Via Cardiotrophin-1. Neuron. 2005;48:253–65.
10. Cahoy JD, Emery B, Kaushal A, Foo LC, Zamanian JL, Christopherson KS, et al. A Transcriptome Database For Astrocytes, Neurons, And Oligodendrocytes: A New Resource For Understanding Brain Development And Function. J Neurosci Off J Soc Neurosci. 2008;28:264–78.
11. Escartin C, Galea E, Lakatos A, O'Callaghan JP, Petzold GC, Serrano-Pozo A, et al. Reactive Astrocyte Nomenclature, Definitions, And Future Directions. Nat Neurosci. 2021;24:312–25.
12. Nishiyama A, Suzuki R, Zhu X. Ng2 Cells (Polydendrocytes) In Brain Physiology And Repair. Front Neurosci. 2014;8:133.
13. Un nuevo proceder para la impregnación de la neuroglia [A new procedure for the impregnation of neuroglia]. Boletín de la Sociedad Española de Biologia. 2:104–8.
14. Schober AL, Wicki-Stordeur LE, Murai KK, Swayne LA. Foundations And Implications Of Astrocyte Heterogeneity During Brain Development And Disease. Trends Neurosci. 2022;45:692–703.
15. Fan Y-Y, Huo J. A1/A2 Astrocytes In Central Nervous System Injuries And Diseases: Angels Or Devils? Neurochem Int. 2021;148: 105080.
16. Rodríguez-Giraldo M, González-Reyes RE, Ramírez-Guerrero S, Bonilla-Trilleras CE, Guardo-Maya S, Nava-Mesa MO. Astrocytes as a Therapeutic Target in Alzheimer's Disease-Comprehensive Review and Recent Developments. Int J Mol Sci. 2022;23:13630.
17. Šerý O, Goswami N, Balcar VJ. Chapter 4 - CD36 gene polymorphisms and Alzheimer's disease. In: Martin CR, Preedy VR, editors. Genet Neurol Behav Diet Dement. Academic Press; 2020. p. 57–70. Available from: https://www.sciencedirect.com/science/article/pii/B9780128158685000049. Cited 2024 Jun 20.
18. Krencik R, Zhang S-C. Directed Differentiation of Functional Astroglial Subtypes from Human Pluripotent Stem Cells. Nat Protoc. 2011;6:1710–7.
19. Tyzack G, Lakatos A, Patani R. Human Stem Cell-Derived Astrocytes: Specification and Relevance for Neurological Disorders. Curr Stem Cell Rep. 2016;2:236–47.
20. Tcw J, Wang M, Pimenova AA, Bowles KR, Hartley BJ, Lacin E, et al. An Efficient Platform for Astrocyte Differentiation from Human Induced Pluripotent Stem Cells. Stem Cell Rep. 2017;9:600–14.
21. Foo LC, Allen NJ, Bushong EA, Ventura PB, Chung W-S, Zhou L, et al. Development of a Novel Method for the Purification and Culture of Rodent Astrocytes. Neuron. 2011;71:799–811.
22. Magistri M, Khoury N, Mazza EMC, Velmeshev D, Lee JK, Bicciato S, et al. A Comparative Transcriptomic Analysis Of Astrocytes Differentiation From Human Neural Progenitor Cells. Eur J Neurosci. 2016;44:2858–70.
23. Perriot S, Mathias A, Perriard G, Canales M, Jonkmans N, Merienne N, et al. Human Induced Pluripotent Stem Cell-Derived Astrocytes Are Differentially Activated by Multiple Sclerosis-Associated Cytokines. Stem Cell Rep. 2018;11:1199–210.
24. Perriot S, Canales M, Mathias A, Du Pasquier R. Differentiation of functional astrocytes from human-induced pluripotent stem cells in chemically defined media. STAR Protoc. 2021;2: 100902.
25. Zhang Y, Sloan SA, Clarke LE, Caneda C, Plaza CA, Blumenthal PD, et al. Purification and Characterization of Progenitor and Mature Human Astrocytes Reveals Transcriptional and Functional Differences with Mouse. Neuron. 2016;89:37–53.
26. Bonni A, Sun Y, Nadal-Vicens M, Bhatt A, Frank DA, Rozovsky I, et al. Regulation of gliogenesis in the central nervous system by the JAK-STAT signaling pathway. Science. 1997;278:477–83.
27. Chandrasekaran A, Avci HX, Leist M, Kobolák J, Dinnyés A. Astrocyte Differentiation of Human Pluripotent Stem Cells: New Tools for Neurological Disorder Research. Front Cell Neurosci. 2016;10:215.
28. Mulica P, Venegas C, Landoulsi Z, Badanjak K, Delcambre S, Tziortziou M, et al. Comparison Of Two Protocols For The Generation Of Ipsc-Derived Human Astrocytes. Biol Proced Online. 2023;25:26.
29. Szeky B, Feher A, Zana M, Kucera R, Lochman J, Dinnyes A. Differentiation of Astrocytes from Human iPSC-derived NPCs. protocols.io. 2024. https://doi.org/10.17504/protocols.io.x54v9pb4mg3e/v1
30. Chambers SM, Fasano CA, Papapetrou EP, Tomishima M, Sadelain M, Studer L. Highly Efficient Neural Conversion Of Human Es And Ips Cells By Dual Inhibition Of Smad Signaling. Nat Biotechnol. 2009;27:275–80.
31. Zhou S, Szczesna K, Ochalek A, Kobolák J, Varga E, Nemes C, et al. Neurosphere Based Differentiation of Human iPSC Improves Astrocyte Differentiation. Stem Cells Int. 2016;2016:4937689.
32. Chandrasekaran A, Avci HX, Ochalek A, Rösingh LN, Molnár K, László L, et al. Comparison Of 2d And 3d Neural Induction Methods For The Generation Of Neural Progenitor Cells From Human Induced Pluripotent Stem Cells. Stem Cell Res. 2017;25:139–51.
33. Santos R, Vadodaria KC, Jaeger BN, Mei A, Lefcochilos-Fogelquist S, Mendes APD, et al. Differentiation of Inflammation-Responsive Astrocytes from Glial Progenitors Generated from Human Induced Pluripotent Stem Cells. Stem Cell Rep. 2017;8:1757–69.
34. Kucera J, Lochman J, Bouchal P, Pakostova E, Mikulasek K, Hedrich S, et al. A Model of Aerobic and Anaerobic Metabolism of Hydrogen in the Extremophile Acidithiobacillus ferrooxidans. Front Microbiol. 2020;11: 610836.
35. Babraham Bioinformatics - FastQC A Quality Control tool for High Throughput Sequence Data. Available from: https://www.bioinformatics.babraham.ac.uk/projects/fastqc/. Cited 2023 Nov 28.
36. FelixKrueger/TrimGalore: v0.6.7 - DOI via Zenodo. Available from: https://zenodo.org/records/5127899. Cited 2023 Nov 28.
37. Wei Z, Zhang W, Fang H, Li Y, Wang X. Esatac: An Easy-To-Use Systematic Pipeline For Atac-Seq Data Analysis. Bioinformatics. 2018;34:2664–5.
38. Morgan M, Pagès H, Obenchain V, Hayden N, Samuel B, Maintainer BP. Rsamtools: Binary alignment (BAM), FASTA, variant call (BCF), and tabix file import. Bioconductor version: Release (3.18); 2023;8. Available from: https://bioconductor.org/packages/Rsamtools/. Cited 2023 Nov 2.
39. Love MI, Huber W, Anders S. Moderated Estimation Of Fold Change And Dispersion For Rna-Seq Data With Deseq2. Genome Biol. 2014;15:550.
40. Suzuki R, Shimodaira H. S. Bioinforma Oxf Engl. 2006;22:1540–2.
41. Galili T. dendextend: an R package for visualizing, adjusting and comparing trees of hierarchical clustering. Bioinformatics. 2015;31:3718–20.
42. Fu R, Gillen AE, Sheridan RM, Tian C, Daya M, Hao Y, et al. clustifyr: an R package for automated single-cell RNA sequencing cluster classification. F1000Research. 2020;9:223.
43. Nowakowski TJ, Bhaduri A, Pollen AA, Alvarado B, Mostajo-Radji MA, Di Lullo E, et al. Spatiotemporal Gene Expression Trajectories Reveal Developmental Hierarchies Of The Human Cortex. Science. 2017;358:1318–23.
44. Sutton GJ, Poppe D, Simmons RK, Walsh K, Nawaz U, Lister R, et al. Comprehensive Evaluation Of Deconvolution Methods For Human Brain Gene Expression. Nat Commun. 2022;13:1358.
45. Hunt GJ, Freytag S, Bahlo M, Gagnon-Bartsch JA. Dtangle: Accurate And Robust Cell Type Deconvolution. Bioinformatics. 2019;35:2093–9.
46. Nagy C, Maitra M, Tanti A, Suderman M, Théroux J-F, Davoli MA, et al. Single-Nucleus Transcriptomics Of The Prefrontal Cortex In Major Depressive Disorder Implicates Oligodendrocyte Precursor Cells And Excitatory Neurons. Nat Neurosci. 2020;23:771–81.

47. Gu Z. Complex heatmap visualization. Imeta. 2022;1:e43.
48. Celá A, Mádr A, Ješeta M, Žáková J, Crha I, Glatz Z. Study Of Metabolic Activity Of Human Embryos Focused On Amino Acids By Capillary Electrophoresis With Light-Emitting Diode-Induced Fluorescence Detection. Electrophoresis. 2018;39:3040–8.
49. Palm T, Bolognin S, Meiser J, Nickels S, Träger C, Meilenbrock R-L, et al. Rapid And Robust Generation Of Long-Term Self-Renewing Human Neural Stem Cells With The Ability To Generate Mature Astroglia. Sci Rep. 2015;5:16321.
50. Shaltouki A, Peng J, Liu Q, Rao MS, Zeng X. Efficient Generation of Astrocytes from Human Pluripotent Stem Cells in Defined Conditions. Stem Cells. 2013;31:941–52.
51. Deloulme JC, Raponi E, Gentil BJ, Bertacchi N, Marks A, Labourdette G, et al. Nuclear Expression Of S100b In Oligodendrocyte Progenitor Cells Correlates With Differentiation Toward The Oligodendroglial Lineage And Modulates Oligodendrocytes Maturation. Mol Cell Neurosci. 2004;27:453–65.
52. Brozzi F, Arcuri C, Giambanco I, Donato R. S100B Protein Regulates Astrocyte Shape and Migration via Interaction with Src Kinase: IMPLICATIONS FOR ASTROCYTE DEVELOPMENT, ACTIVATION. AND TUMOR GROWTH J Biol Chem. 2009;284:8797–811.
53. Crowe EP, Tuzer F, Gregory BD, Donahue G, Gosai SJ, Cohen J, et al. Changes in the Transcriptome of Human Astrocytes Accompanying Oxidative Stress-Induced Senescence. Front Aging Neurosci. 2016;8. Available from: https://www.frontiersin.org/articles/https://doi.org/10.3389/fnagi.2016.00208. Cited 2023 Jan 1.
54. Bradley RA, Shireman J, McFalls C, Choi J, Canfield SG, Dong Y, et al. Regionally specified human pluripotent stem cell-derived astrocytes exhibit different molecular signatures and functional properties. Dev Camb Engl. 2019;146. Available from: https://www.ncbi.nlm.nih.gov/pmc/articles/PMC6633609/. Cited 2023 Dec 1.
55. Yoo HC, Yu YC, Sung Y, Han JM. Glutamine reliance in cell metabolism. Exp Mol Med. 2020;52:1496–516.
56. Sullivan LB, Gui DY, Hosios AM, Bush LN, Freinkman E, Vander Heiden MG. Supporting Aspartate Biosynthesis Is an Essential Function of Respiration in Proliferating Cells. Cell. 2015;162:552–63.
57. Salcedo C, Andersen JV, Vinten KT, Pinborg LH, Waagepetersen HS, Freude KK, et al. Functional Metabolic Mapping Reveals Highly Active Branched-Chain Amino Acid Metabolism in Human Astrocytes, Which Is Impaired in iPSC-Derived Astrocytes in Alzheimer's Disease. Front Aging Neurosci. 2021;13. Available from: https://www.frontiersin.org/articles/https://doi.org/10.3389/fnagi.2021.736580. Cited 2024 Feb 27.
58. SubbiahanadarChelladurai K, SelvanChristyraj JD, Rajagopalan K, Yesudhason BV, Venkatachalam S, Mohan M, et al. Alternative To Fbs In Animal Cell Culture - An Overview And Future Perspective. Heliyon. 2021;7:e07686.
59. Fathi A, Eisa-Beygi S, Baharvand H. Signaling Molecules Governing Pluripotency and Early Lineage Commitments in Human Pluripotent Stem Cells. Cell J. 2017;19:194–203.
60. Mossahebi-Mohammadi M, Quan M, Zhang J-S, Li X. FGF Signaling Pathway: A Key Regulator of Stem Cell Pluripotency. Front Cell Dev Biol. 2020;8. Available from: https://www.frontiersin.org/articles/https://doi.org/10.3389/fcell.2020.00079. Cited 2023 Dec 11.
61. Siani A, Khaw RR, Manley OWG, Tirella A, Cellesi F, Donno R, et al. Fibronectin Localization And Fibrillization Are Affected By The Presence Of Serum In Culture Media. Sci Rep. 2015;5:9278.
62. Pot SA, Lin Z, Shiu J, Benn MC, Vogel V. Growth Factors And Mechano-Regulated Reciprocal Crosstalk With Extracellular Matrix Tune The Keratocyte–Fibroblast/Myofibroblast Transition. Sci Rep. 2023;13:11350.
63. Pellegrin S, Mellor H. The Rho Family Gtpase Rif Induces Filopodia Through Mdia2. Curr Biol CB. 2005;15:129–33.
64. Schiweck J, Eickholt BJ, Murk K. Important Shapeshifter: Mechanisms Allowing Astrocytes to Respond to the Changing Nervous System During Development. Injury and Disease Front Cell Neurosci. 2018;12:261.
65. Wiese S, Karus M, Faissner A. Astrocytes as a Source for Extracellular Matrix Molecules and Cytokines. Front Pharmacol. 2012;3. Available from: https://www.frontiersin.org/articles/https://doi.org/10.3389/fphar.2012.00120. Cited 2023 Dec 4.
66. Allnoch L, Leitzen E, Zdora I, Baumgärtner W, Hansmann F. Astrocyte Depletion Alters Extracellular Matrix Composition In The Demyelinating Phase Of Theiler's Murine Encephalomyelitis. PLoS ONE. 2022;17:e0270239.
67. Woo AM, Sontheimer H. Interactions Between Astrocytes And Extracellular Matrix Structures Contribute To Neuroinflammation-Associated Epilepsy Pathology. Front Mol Med. 2023;3:1198021.
68. Dyck SM, Karimi-Abdolrezaee S. Chondroitin Sulfate Proteoglycans: Key Modulators In The Developing And Pathologic Central Nervous System. Exp Neurol. 2015;269:169–87.
69. Clarke SR, Shetty AK, Bradley JL, Turner DA. Reactive Astrocytes Express The Embryonic Intermediate Neurofilament Nestin. NeuroReport. 1994;5:1885–8.
70. Liu Z, Li Y, Cui Y, Roberts C, Lu M, Wilhelmsson U, et al. Beneficial Effects Of Gfap/Vimentin Reactive Astrocytes For Axonal Remodeling And Motor Behavioral Recovery In Mice After Stroke. Glia. 2014;62:2022–33.
71. Raskatov JA. What is the "Relevant" Amyloid β 42 Concentration? Chembiochem Eur J Chem Biol. 2019;20:1725–6.
72. Shannon P, Markiel A, Ozier O, Baliga NS, Wang JT, Ramage D, et al. Cytoscape: A Software Environment for Integrated Models of Biomolecular Interaction Networks. Genome Res. 2003;13:2498–504.
73. Basu A, Jain N, Tolbert BS, Komar AA, Mazumder B. Conserved Structures Formed By Heterogeneous Rna Sequences Drive Silencing Of An Inflammation Responsive Post-Transcriptional Operon. Nucleic Acids Res. 2017;45:12987–3003.
74. Poddar D, Kaur R, Baldwin WM, Mazumder B. L13a-Dependent Translational Control In Macrophages Limits The Pathogenesis Of Colitis. Cell Mol Immunol. 2016;13:816–27.
75. Semyanov A, Verkhratsky A. Astrocytic Processes: From Tripartite Synapses To The Active Milieu. Trends Neurosci. 2021;44:781–92.
76. Kim J, Yoo ID, Lim J, Moon J-S. S. Exp Mol Med. 2024;56:95–9.
77. Preman P, Alfonso-Triguero M, Alberdi E, Verkhratsky A, Arranz AM. Astrocytes in Alzheimer's Disease: Pathological Significance and Molecular Pathways. Cells. 2021;10:540.
78. Dai S, Qiu L, Veeraraghavan VP, Sheu CL, Mony U. Advances in iPSC technology in neural disease modeling, drug screening, and therapy. Curr Stem Cell Res Ther. 2024;19(6):809–19. https://doi.org/10.2174/1574888x18666230608105703.
79. Penney J, Ralvenius WT, Tsai L-H. Modeling Alzheimer's Disease With Ipsc-Derived Brain Cells. Mol Psychiatry. 2020;25:148–67.
80. Emdad L, D'Souza SL, Kothari HP, Qadeer ZA, Germano IM. Efficient Differentiation Of Human Embryonic And Induced Pluripotent Stem Cells Into Functional Astrocytes. Stem Cells Dev. 2012;21:404–10.
81. Jones VC, Atkinson-Dell R, Verkhratsky A, Mohamet L. Aberrant Ipsc-Derived Human Astrocytes In Alzheimer's Disease. Cell Death Dis. 2017;8:e2696.
82. Roybon L, Lamas NJ, Garcia-Diaz A, Yang EJ, Sattler R, Jackson-Lewis V, et al. Human Stem Cell-Derived Spinal Cord Astrocytes With Defined Mature Or Reactive Phenotypes. Cell Rep. 2013;4:1035–48.
83. Pozzi D, Ban J, Iseppon F, Torre V. An Improved Method For Growing Neurons: Comparison With Standard Protocols. J Neurosci Methods. 2017;280:1–10.
84. Hung C-H, Young T-H. Differences In The Effect On Neural Stem Cells Of Fetal Bovine Serum In Substrate-Coated And Soluble Form. Biomaterials. 2006;27:5901–8.
85. Li Y-C, Lin Y-C, Young T-H. Combination Of Media, Biomaterials And Extracellular Matrix Proteins To Enhance The Differentiation Of Neural Stem/Precursor Cells Into Neurons. Acta Biomater. 2012;8:3035–48.
86. Lundin A, Delsing L, Clausen M, Ricchiuto P, Sanchez J, Sabirsh A, et al. Human iPS-Derived Astroglia from a Stable Neural Precursor State Show Improved Functionality Compared with Conventional Astrocytic Models. Stem Cell Rep. 2018;10:1030–45.
87. Oh LY, Yong VW. Astrocytes Promote Process Outgrowth By Adult Human Oligodendrocytes In Vitro Through Interaction Between Bfgf And Astrocyte Extracellular Matrix. Glia. 1996;17:237–53.
88. Shea TB, Beermann ML, Honda T, Nixon RA. Secretion Of Amyloid Precursor Protein And Laminin By Cultured Astrocytes Is Influenced By Culture Conditions. J Neurosci Res. 1994;37:197–207.

89. van der Laan LJ, De Groot CJ, Elices MJ, Dijkstra CD. Extracellular Matrix Proteins Expressed By Human Adult Astrocytes In Vivo And In Vitro: An Astrocyte Surface Protein Containing The Cs1 Domain Contributes To Binding Of Lymphoblasts. J Neurosci Res. 1997;50:539–48.
90. Novo M, Freire S, Al-Soufi W. Critical aggregation concentration for the formation of early Amyloid-β (1–42) oligomers. Sci Rep. 2018;8:1783.

Publisher's Note